Optimising the Structural Properties of Bio-based Cob Materials

Kamal HADDAD[1*][0000-0003-1264-9563], Simon LANNON[2][0000-0003-4677-7184], Eshrar LATIF[2][0000-0003-3982-6929]

[1] Amman Arab University, Al-Urdon St., 11941, Jordan
[2] Cardiff University, Cardiff CF10 3AT, United Kingdom
K.haddad@aau.edu.jo

Abstract. Conventional construction materials such as concrete and steel carry high environmental costs, intensifying the need for lower-impact alternatives. Cob, an earthen composite of subsoil, water, and natural fibres, offers potential as a low-energy construction material, but its mechanical performance and dimensional stability remain insufficiently quantified for consistent structural use. This study examined how fibre type, fibre dosage, and initial water content influence the compressive behaviour and shrinkage response of bio-based cob mixes, with the aim of establishing repeatable composition–property relationships within the tested system.

A multi-stage experimental framework was implemented. Subsoil grading was characterised by dry sieving, and fibre length distributions for barley straw and hemp shiv were quantified using computational machine vision. Based on these characterisations, 51 cob mixes were produced with controlled variations in fibre type, fibre dosage, and water content. Material-scale testing quantified dry bulk density, volumetric shrinkage, shrinkage ratio, and compressive strength (n = 3 per mix). A dedicated variability experiment evaluated the influence of fabrication controls and informed a refined protocol to improve repeatability. Ten optimised mixes were then assessed under standardised placement and consolidation into moulds and controlled drying.

Organic fibres improved compressive response and shrinkage control, although the relationships were non-linear. Across the test matrix, compressive strength reached 1.58 MPa, while volumetric shrinkage increased up to 27.1% when initial water content and fibre dosage were excessive. In the final evaluation set, mixes with 20–25% initial water and moderate total fibre achieved the most consistent balance between strength and dimensional stability, with higher hemp-to-straw proportions generally outperforming straw-rich compositions. Mix H6S1W25 (6% hemp shiv, 1% barley straw, 25% water) delivered the highest overall structural performance within the tested set. These outcomes provide empirically grounded benchmarks for specimen-scale cob mix optimisation under controlled fabrication conditions.

Keywords: Structural Properties, Circular Construction, Bio-based, Earthen materials, Sustainable materials.

1 Introduction

The construction sector faces increasing scrutiny due to the environmental burden of conventional materials such as concrete and steel. Cement production alone is responsible for approximately 8% of global CO_2 emissions [1], and the wider construction sector accounts for 30% of global final energy consumption and 27% of energy sector emissions, underscoring the urgent need for lower-impact alternatives [2].

In this context, geo-based and bio-based materials such as cob are being revisited as circular, low-carbon construction options [3]. Cob is a monolithic earthen material composed of subsoil, water, and natural fibres; earthen construction techniques generally require less energy in production and use, and therefore reduce greenhouse gas emissions [4]. Cob offers advantages in workability and architectural flexibility compared to techniques such as rammed earth and adobe[5].

However, despite its environmental potential, cob remains insufficiently optimised in mechanical and dimensional terms. Cob typically exhibits lower compressive strength than other earthen materials [6], where its performance depends strongly on its constituents. In particular, structural cohesion and tensile capacity derive largely from the inclusion of organic fibres, which act as reinforcement [7]. Yet few studies establish quantitative links between mix composition, strength, and dimensional stability. This limits broader adoption of cob as a structurally reliable construction material.

This investigation aims to address this knowledge gap by detailing the optimisation of the structural properties of bio-based cob materials. Ultimately, this paper outlines the process of developing and validating structurally viable cob compositions, providing empirical benchmarks for researchers and practitioners evaluating cob as a structurally reliable, low-energy construction material.

2 Literature Review

Cob has lower compressive strength than other earthen materials but provides adequate shear resistance[8]. As it dries, its compressive strength increases during drying, and its tensile capacity comes mainly from organic fibres that improve cohesion [9]. Cob can also endure stresses beyond its peak strength, deforming plastically past the elastic limit with a gradual decrease in load-bearing capacity [10]. This section covers an overview of the structural testing performed on cob with a focus on compressive strength, volumetric shrinkage, and shrinkage ratio.

Reported compressive strengths for cob vary widely. Vinceslas et al. tested fibre-reinforced cob walls prepared using a vernacular process and found uniaxial compressive strengths between 0.50 MPa and 0.76 MPa, with denser specimens showing higher strength but lower stiffness [11, 12]. Miccoli et al. measured strengths between 1.55 MPa and 1.63 MPa at a loading rate of 0.25 mm/min, reaching failure within 15-30 minutes [8, 10].

Other studies have shown strong sensitivity to moisture content, fibre type, and stabilisation: Saxton reported 0.35-1.75 MPa at 15% water content [13]; Sangma and Tripura reported 1.35-2.98 MPa in cement-stabilised mixes, 1.25-1.63 MPa with coconut coir, and 1.18-1.34 MPa with straw [7]; Wright found 0.77-2.45 MPa depending on straw content and soil-clay ratio [14]; Houben and Guillaud in addition to Quagliarini et al. reported lower values of 0.10 MPa and 0.24-0.40 MPa, respectively

[15, 16]. Following DIN 18945, Miccoli et al. achieved a mean compressive strength of 1.59 MPa with a standard deviation of 0.03 MPa [8].

Dimensional stability is governed by drying behaviour. Shrinkage and cracking in cob arise mainly from volumetric contraction as water evaporates, and are strongly affected by fibre content, water content, and particle size distribution [8, 13]. Saxton observed that higher straw content, which requires higher initial water for workability, led to greater shrinkage [13]. Sangma and Tripura reported linear shrinkage between 3.18% and 6.46% depending on moulding water (31.7-40%) and drying temperature (30-70°C); adding 3% coir or 3% straw reduced shrinkage to around 1.07-1.31%, while mixes with 10% fibre shrank by 1.69% at 70°C [17].

Tchiotsop et al. measured volumetric shrinkage of 13.07 ± 0.12% in non-fibred cob; 16-17% in cob with flax yarn; 12-17% in cob with hemp shiv; and as low as 5.13 ± 0.45% with 3% hay stalks [18]. Vinceslas et al., following Hamard et al., also quantified anisotropy using the shrinkage ratio, defined as the ratio of vertical to horizontal shrinkage, and concluded that cob walls had the highest shrinkage ratios. [11, 12].

Cob exhibits variable compressive strength and is vulnerable to drying-induced shrinkage and anisotropic deformation, both of which are governed by water content, fibre type, and fibre dosage. Addressing these coupled mechanical and dimensional behaviours is central to this paper, which aims to define cob mix designs that are not only strong enough for load-bearing use but also sufficiently dimensionally stable to be viable in contemporary construction.

3 Materials and Methods

The study investigated the structural performance of cob, a bio-based construction material composed of subsoil, water, and natural fibres. Two fibrous reinforcements were examined: barley straw and hemp shiv. The subsoil was collected from a farm in Cardiff, UK, at depths of 60-120 cm to reduce biological contamination and ensure uniform mineral composition. The overarching aim was to optimise cob's mechanical performance by establishing clear relationships between constituent composition, fabrication procedure, and resulting structural properties.

Particle size distribution by dry sieving followed EN 12620:2002+A1:2008 using the sieving procedure in EN 933-1:2012. Compressive strength testing followed EN 12390-3:2019. Dry bulk density was calculated in accordance with ISO 10545-3:1995. Volumetric shrinkage was calculated using a wet-to-dry volume ratio based on mould volume and dried specimen dimensions.

Cube specimens (100 mm × 100 mm × 100 mm) were rotated 45° and tested in uniaxial compression in accordance with EN 12390-3:2019. A continuous and uniform load was applied at a controlled rate of 0.0013 cm/s until failure, and compressive strength was calculated as the maximum recorded load divided by the measured cross-sectional area. Results were averaged across three replicate specimens per mix.

The specimen mass (M) was measured using a scale with a precision of ±0.01 g, and the specimen dimensions were measured using a ruler with a precision of ±0.5

mm to determine the volume (V). Dry bulk density (ρ)was calculated as $\rho = M/V$in accordance with ISO 10545-3:1995.

Finally, volumetric shrinkage was calculated as the ratio between specimen volume in the dry state and specimen volume when cast in the mould, expressed as Volumetric Shrinkage $= (V_{dry}/V_{wet}) \times 100\%$, where $V_{wet}$is the mould volume (0.001 m³ for a 100 mm cube). Meanwhile, the

shrinkage ratio (H/V) was calculated as the ratio of vertical shrinkage to horizontal shrinkage, where vertical shrinkage is the change in specimen height and horizontal shrinkage is the mean change in the two orthogonal plan dimensions.

At the constituent level, sieve analysis was conducted to limit coarse inclusions (e.g., gravel-sized particles) and standardise the maximum particle size for laboratory specimens, thereby reducing variability between mixes. A series of sieves ranging from 6 mm to 90 µm was used in descending order and secured within a mechanical sieve shaker for 5 ± 1 minutes to ensure effective separation without particle degradation. Conventional sieve testing, however, proved unsuitable for fibres because of their nature, preventing them from passing through the sieves. To address this, a machine-vision algorithm was developed in Python to analyse top-view images of hemp and straw fibres captured using a high-resolution camera, as shown in Figure 1. The algorithm applied binary thresholding to determine fibre length distributions. This digital method provided a quantitative description of fibre morphology used to support interpretation of mechanical trends. Any relationship between fibre length and cohesion/strength is treated as an interpretation in this paper and would require dedicated correlation analysis to confirm.

(A) (B)

Figure 1. (A) Captured image of a hemp shiv sample (B) Binary analysis of the sample to identify the fibre size distribution.

Then, four primary mix categories were developed to explore the influence of fibre type and dosage. The first incorporated hemp shiv at 1-10% by mass relative to dry subsoil mass, the second used barley straw at the same range, and the third combined both fibres with a total fibre content not exceeding 10%. This range was used as a sensitivity range to map non-linear trends and identify an optimum within the tested system, rather than as a recommended practice dosage. The fourth category contained no fibre and served as the control. Each mix was tested with water contents of 20%, 25%, and 30% to assess the interaction between moisture level and mechanical behaviour. H% and S% represent the mass of dry fibre expressed as a percentage of the mass of dry subsoil. W% represents gravimetric water content, defined as $W = (m_{water}/m_{dry\ subsoil}) \times 100\%$. All reported percentages in this paper are on a mass basis unless otherwise stated.

Atterberg limits (LL/PL/PI) were not measured for the subsoil used in this paper; therefore, the mixture states are reported operationally as hand-formable cob mixes suitable for mould casting rather than classified as plastic or liquid. The sensitivity testing revealed notable variability in results, prompting a dedicated experiment to evaluate how preparation methods affected performance consistency. Mixes were selected based on the standard deviation of their initial strength results. The refined protocol introduced several controls: oven drying replaced ambient drying, plastic moulds substituted timber ones to avoid moisture absorption, and soil preparation and mixing procedures were standardised to ensure uniformity. Specimens were dried in a temperature-controlled oven at 40 °C for 72 hours, with mass monitored to assess drying progression.

In this paper, consolidation refers to the controlled placement of fresh cob into 100 mm cube moulds to standardise density and reduce voids. Fresh cob was placed in approximately 4 cm layers and consolidated with a hand rammer before the next layer was applied.

In the final testing phase, nine optimised cob mixes were produced and evaluated alongside the best-performing mix from the earlier stages. Structural assessment focused on compressive strength, dry bulk density, volumetric shrinkage, and shrinkage ratio. Compressive strength was prioritised as the primary performance criterion, reflecting cob's typical application in monolithic wall systems dominated by compressive loading. Tensile and flexural properties were not examined, as these stresses are generally limited in traditional cob construction.

The insights gained informed ten refined mixes for the final performance evaluation. These designs prioritised hemp, favoured 20-25% water to reduce scatter, and retained some 30% variants for comparison. H7W20, the best single-fibre performer, served as a benchmark. Table 1 lists the fibre and water proportions, with subsoil forming the remainder.

Table 1. The proposed mixes and their content in (%) for the performance evaluation phase.

Mix ID	Water Content (W)	Hemp shiv (H)	Barley Straw (S)
Mix H6S1W25	25	6	1
Mix H8S1W30	30	8	1
Mix H7S2W20	20	7	2
Mix H5S1W25	25	5	1
Mix H9S3W20	20	9	3
Mix H10S2W25	25	10	2
Mix H6S3W30	30	6	3
Mix H8S4W20	20	8	4
Mix H5S2W30	30	5	2
Mix H7W20	20	7	0

4 Results and Discussion

4.1 Constituents Characterisation

Sieve testing was used to characterise the coarse-to-fine grading of the subsoil within the tested range (6 mm to 90 µm) and to inform consistent specimen preparation (maximum particle size control) by limiting coarse inclusions. The results are presented as mass percentage retained on each sieve size (Figure 2). Material passing the 90 µm sieve is reported as a single combined fraction (<90 µm). This retained-mass presentation provides a clear description of the distribution across the sieve series used; however, it does not resolve particle-size differentiation within the <90 µm fraction and therefore cannot be used to infer a definitive soil textural class from fines alone.

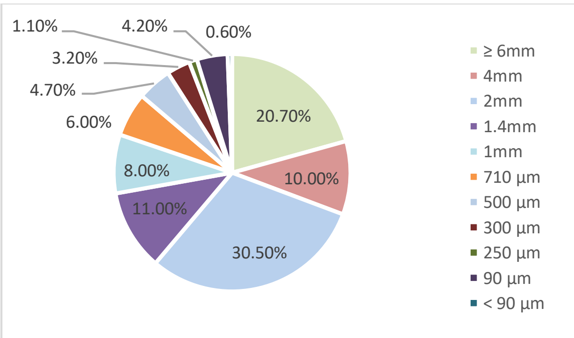

Figure 2. Subsoil grading expressed as mass percentage retained on each sieve size (dry sieving, 6 mm to 90 µm). Material passing 90 µm is reported as a combined <90 µm fraction.

In parallel, the use of the machine vision algorithm demonstrated that hemp shiv particles were primarily below 10 mm in length. In comparison, barley straw fibres ranged between 10 and 30 mm. The results suggest that, within the tested mixes and preparation protocol, hemp shiv mixes often achieved higher compressive strength than straw-only mixes. Fibre morphology is discussed as a plausible contributing factor, but the fibre-size-cohesion relationship is not presented as a proven causal mechanism without dedicated correlation analysis.

4.2 Sensitivity Testing Phase

The 51 trial mixes established clear behavioural trends. The non-fibred control provided the baseline. Bulk density increased from 1653 kg/m^3 at 20% water to 1720 kg/m^3 at 25%, before decreasing to 1605 kg/m^3 at 30%. Meanwhile, volumetric shrinkage followed the opposite trend, with 18.7% at 25% water, 20.4% at 20%, and 21.9% at 30%. Compressive strength mirrored density, peaking at 1.15 MPa at 25% water and declining to 0.97 MPa at 20% and 0.89 MPa at 30%. Therefore, 25% water produced the most favourable combination of placement density, specimen stability, and compressive strength.

Hemp shiv increased compressive strength and generally reduced shrinkage across the tested water levels within this dataset. The strongest results were 1.66 MPa at 10% hemp with 20% water and 1.71 MPa at 1% hemp with 30% water. Meanwhile, the lowest shrinkage, at 16.1%, occurred in the 10% hemp and 25% water mix. Bulk density ranged from 1608 to 1899 kg/m^3, reflecting the balance between fibre-induced porosity and improved particle packing. The observed behaviour is interpreted as being consistent with crack restraint and matrix reinforcement; however, the relationship with fibre content is non-linear.

In contrast, straw behaved differently. Density decreased, yet shrinkage control improved significantly. The minimum shrinkage, 14.9%, was observed in the mix with 7% straw and 30% water. Strength improved only at low straw contents: 1.15 MPa at 1% straw with 25% water, matching the non-fibred maximum. However, higher straw contents reduced strength to between 0.71 and 0.96 MPa, depending on water level. This reduction resulted from increased porosity and diminished cohesion.

Additionally, mixed fibres offered the most balanced performance. The lowest volumetric shrinkage in the entire dataset was 14.2% at 7% hemp and 3% straw with 30% water. Compressive strength ranged from 0.94 to 1.23 MPa, peaking at 1.23 MPa for 1% hemp and 4% straw with 20% water. Densities ranged from 1550 to 1700 kg/m^3, comparable to those of straw-only mixes. These outcomes are consistent with improved crack restraint and load transfer in mixed-fibre systems; however, microstructural network formation is not directly demonstrated in this paper and is treated as an interpretation.

Overall, an initial water content of 25% was the most structurally favourable. In fibred mixes, performance depended on both density and shrinkage. Hemp improved strength through crack-bridging and fibre-matrix interaction effects, while straw restrained shrinkage but reduced strength at higher contents due to increased porosity and reduced packing efficiency. Consequently, blended mixes achieved low shrinkage with sufficient strength, making them strong candidates for load-bearing applications.

4.3 Variability Experiment and Mixes Optimisation

The variability study explored the influence of fabrication methods on performance. Two contrasting mixes were examined: H7S3W30, which had shown stability, and H1W25, which had exhibited cracking and more fluctuant results in the previous stage. These were retested under controlled subsoil preparation, standardised placement and consolidation into moulds, and controlled oven drying to isolate process effects.

Under these conditions, H7S3W30 developed only limited surface cracking, whereas H1W25 displayed extensive cracking, and one specimen failed. Thus, higher fibre contents appeared to improve crack resistance. However, they also increased matrix heterogeneity, potentially hindering uniform load transfer.

Meanwhile, dry bulk density rose for both mixes. H7S3W30 increased from 1566 to 1712 kg/m^3, and H1W25 from 1804 to 1876 kg/m^3. Strength improved in parallel, with H7S3W30 rising from 0.92 to 2.42 MPa (a 163% gain) and H1W25 from 1.66 to 3.00 MPa (an 81% gain). These gains highlight that consolidation consistency (density control) and uniform drying are critical, as they enhance particle contact and reduce weak interfaces.

However, volumetric shrinkage also increased under accelerated drying. H7S3W30 rose from 18.5% to 27.1%, and H1W25 from 20.4% to 34.8%. Straw in H7S3W30 partly restrained deformation, yet rapid moisture loss still generated high internal stress.

Additionally, strength variability increased with higher fibre content. The standard deviation in H7S3W30 grew from 0.04 MPa to 0.44 MPa, whereas H1W25, with less fibre, was more consistent. Fibre-rich cob, therefore, required strict control of mixing and placement to achieve uniform results.

4.4 Performance Evaluation Phase

This phase evaluated volumetric shrinkage, shrinkage ratio, and compressive strength. Together, these indicators describe resistance to deformation and load capacity in monolithic walls. Volumetric shrinkage ranged from 20.1% to 27.1%, and shrinkage ratios from 0.51 to 1.02. The lowest values occurred in H7W20, consisting of 20% water and 7% hemp, with 20.1% shrinkage and a ratio of 0.51. Meanwhile, the highest were found in H5S2W30 with 30% water, 5% hemp, and 2% straw, resulting in 27.1% shrinkage and a ratio of 1.02.

Furthermore, mixes with 30% water, such as H8S1W30 and H6S3W30, showed higher shrinkage, whereas those with 20% water, such as H7S2W20 and H9S3W20, exhibited lower shrinkage. Higher initial moisture increased clay mobility and capillary tension during drying, which raised contraction and cracking risk.

Fibre effects were non-linear and interacted with density. Moderate fibre dosages improved cohesion through micro-reinforcement and crack bridging. Excessive dosages increased porosity and moisture pathways, leading to greater deformation. For instance, H9S3W20 with 12% total fibre recorded 25.2% shrinkage, while H7S2W20, which consists of 9% total fibre, had 24.4%. The difference was modest but confirmed that there is an optimum rather than a linear benefit. Meanwhile, higher dry density reduced shrinkage and data scatter by limiting voids.

Compressive strength ranged from 0.90 to 1.58 MPa and followed density trends. The maximum occurred in H6S1W25, which includes 25% initial water content, 6% hemp shiv, 1% barley straw, which reached 1.58 MPa at 1646 kg/m^3. The minimum was in H6S3W30 with 30% initial water and 9% total fibre, achieving 0.90 MPa at 1509 kg/m^3. At comparable fibre levels, water content remained decisive. H7S2W20 achieved 1.29 MPa, while H10S2W25 reached 0.96 MPa, confirming that higher water content reduced placement density and weakened inter-particle bonding within the tested protocol.

Overall, controlling water content 20-25% and maintaining moderate fibre levels improved packing, stabilised drying, and delivered more reliable compressive capacity.

The optimised mixes achieved compressive strengths comparable to the upper end of the range reported in earlier studies, confirming the material's structural viability. Strength values up to 1.58 MPa were consistent with, and in some cases exceeded, previously established benchmarks. Shrinkage levels were somewhat higher than those reported under controlled laboratory conditions; translation to wall-scale performance and field drying conditions requires further validation. Overall, the results indicate improved dimensional control compared with earlier phases and prior work, supporting the effectiveness of the optimised mix design at the specimen scale. Table 2 presents the results of the bulk density, volumetric shrinkage, shrinkage ratio and compressive strength after applying the refined protocols along with the standard deviations across the different samples of each mix. All reported properties are presented as mean ± SD from three specimens per mix (n = 3).

Table 2. Performance evaluation results of the optimised cob mixes (mean ± SD, n = 3).

Mix ID	Bulk Density (kg/m^3)	Volumetric Shrinkage (%)	Shrinkage ratio (H/V)	Compressive Strength (MPa)
Mix H6S1W25	1646 ± 66	22.2 ± 3.0	0.54 ± 0.27	1.58 ± 0.25
Mix H8S1W30	1548 ± 61	26.6 ± 1.7	0.97 ± 0.19	1.18 ± 0.08
Mix H7S2W20	1622 ± 63	24.4 ± 2.7	0.75 ± 0.27	1.29 ± 0.16
Mix H5S1W25	1601 ± 39	22.4 ± 3.0	0.61 ± 0.26	0.98 ± 0.22
Mix H9S3W20	1626 ± 22	25.2 ± 1.3	0.86 ± 0.12	1.10 ± 0.11
Mix H10S2W25	1546 ± 48	23.2 ± 1.0	0.72 ± 0.07	0.96 ± 0.08
Mix H6S3W30	1509 ± 42	24.6 ± 1.4	0.78 ± 0.15	0.90 ± 0.12
Mix H8S4W20	1574 ± 49	23.0 ± 0.9	0.69 ± 0.06	1.03 ± 0.05
Mix H5S2W30	1634 ± 9	27.1 ± 0.8	1.01 ± 0.06	1.16 ± 0.13
Mix H7W20	1587 ± 61	20.1 ± 2.8	0.51 ± 0.13	0.99 ± 0.20

5 Overall Synthesis

Performance progressively shifted towards stable and reproducible behaviour. In the sensitivity phase, the non-fibred control achieved 1.15 MPa at 25% water. Meanwhile, mixed-fibre combinations produced the lowest shrinkage of 14.2% at 7% hemp and 3% straw with 30% water, although these results involved trade-offs. High straw contents reduced strength, and mixed systems were more sensitive to process variations. During the variability study, strict process control increased the strength to 2.42 MPa and 3.00 MPa. However, shrinkage rose sharply under accelerated drying, and strength variability increased in the fibre-rich mix.

Consequently, the optimised group favoured 20-25% water, moderate total fibre, and a higher proportion of hemp. This adjustment reduced shrinkage compared with 30% water and preserved strength compared with straw-rich compositions. It also accepted slightly higher minimum shrinkage than the best early mixed-fibre results to achieve better mechanical performance under realistic drying and consolidation conditions. H6S1W25 gave the highest strength of 1.58 MPa with moderate shrinkage, whereas H7W20 produced the lowest shrinkage of 20.1% and the smallest ratio of 0.51 with acceptable strength. Together, these two mixes defined the practical balance between dimensional stability and compressive capacity.

Process control emerged as the primary contributor to structural performance. Lower water contents improved packing and density. Moderate hemp levels enhanced crack resistance without undermining cohesion. Meanwhile, limited straw in the range of 1 to 4% helped restrain shrinkage without the strength losses seen at higher straw contents. These findings align with the constituent characterisation and are consistent with the influence of fibre length on structural behaviour.

Additionally, optimisation narrowed performance variability. Strength clustered around 1.0-1.6 MPa, while shrinkage remained between 20% and 27%. This stability avoided reliance on exceptional or fragile results.

6 Conclusion

This study integrated diverse results into a practical framework for structural cob. The synthesis showed that density governed performance, while water content and fibre proportion were controllable factors shaping density and pore structure. Mixes with limited water and moderate fibre contents formed compact microstructures, reduced shrinkage, and delivered reliable compressive strength. Hemp shiv improved crack control with minimal loss of strength, whereas high straw contents exchanged shrinkage restraint for increased porosity. Sample preparation management enhanced these gains by stabilising placement/consolidation into moulds and drying.

The main contribution was an actionable optimisation logic at the specimen scale. Within the tested soil, fibres, and preparation protocol, a practical balance was achieved by specifying 20-25% initial water, prioritising hemp over straw, and maintaining uniform mixing, placement/consolidation into moulds, and controlled drying. The optimisation also clarified trade-offs: slightly higher minimum shrinkage was accepted when it improved the consistency of compressive strength within the tested set.

It is essential to highlight that the results are based on laboratory cube specimens and do not directly represent wall-scale behaviour. Atterberg limits were not measured for the tested subsoil. Workability validation with practitioners was not included. These limitations define the priority scope for future work.

Overall, the work defines a clear route from constituent selection to structural adequacy. It links composition, process control, and density to more repeatable strength and shrinkage outcomes within the tested set, positioning cob as a credible low-energy material. Future research should integrate thermal and hygric targets with structural parameters to co-optimise environmental and mechanical performance at the building scale.

References

1. Chandler, D.L. *Researchers have created emissions-free cement*. Climate Change 2019 [cited 2025 09/12]; Available from: https://www.weforum.org/agenda/2019/09/cement-production-country-world-third-largest-emitter/.
2. IEA. *Global Energy Review: CO2 Emissions in 2021*. 2022 [cited 2025 02/12]; Available from: https://www.iea.org/reports/global-energy-review-co2-emissions-in-2021-2.
3. MacDougall, C., *Natural building materials in mainstream construction: Lessons from the UK.* Journal of Green Building, 2008. **3**(3): p. 1-14.
4. Al-Jokhadar, A. and Y. Soudi. *Potentials of Constructing Sustainable Rammed Earth Buildings in Hot-Arid Regions: Structural and Environmental Challenges*. in *Proceedings of the International Conference of Contemporary Affairs in Architecture and Urbanism-ICCAUA*. 2023.
5. Gomaa, M., et al., *Feasibility of 3DP cob walls under compression loads in low-rise construction.* Construction and Building Materials, 2021. **301**: p. 124079.
6. Gomaa, M., et al., *Digital manufacturing for earth construction: A critical review.* Journal of Cleaner Production, 2022. **338**: p. 130630.
7. Sangma, S. and D.D. Tripura, *Characteristic properties of unstabilized, stabilized and fibre-reinforced cob blocks.* Structural Engineering International, 2021. **31**(1): p. 76-84.
8. Miccoli, L., et al., *Static behavior of cob: Experimental testing and finite-element modeling.* Journal of Materials in Civil Engineering, 2019. **31**(4): p. 04019021.
9. Veliz Reyes, A., et al., *Negotiated matter: a robotic exploration of craft-driven innovation.* Architectural Science Review, 2019. **62**(5): p. 398-408.
10. Miccoli, L., U. Müller, and P. Fontana, *Mechanical behaviour of earthen materials: A comparison between earth block masonry, rammed earth and cob.* Construction and building materials, 2014. **61**: p. 327-339.
11. Vinceslas, T., et al., *Further development of a laboratory procedure to assess the mechanical performance of cob.* Environmental Geotechnics, 2018. **7**(3): p. 200-207.
12. Hamard, E., et al., *A new methodology to identify and quantify material resource at a large scale for earth construction-Application to cob in Brittany.* Construction and Building materials, 2018. **170**: p. 485-497.
13. Saxton, R., *Performance of cob as a building material.* Structural Engineer, 1995. **73**(7): p. 111-115.
14. Wright, D.J., *Building from the Ground Up: Understanding and Predicting the Strength of Cob, an Earthen Construction Material*. 2019: The University of Tulsa.
15. Houben, H. and H. Guillaud, *Earth construction: a comprehensive guide*. 1994.
16. Quagliarini, E., et al., *Cob construction in Italy: Some lessons from the past.* Sustainability, 2010. **2**(10): p. 3291-3308.
17. Sangma, S. and D.D. Tripura, *Experimental study on shrinkage behaviour of earth walling materials with fibers and stabilizer for cob building.* Construction and Building Materials, 2020. **256**.
18. Tchiotsop, J., et al., *Assessment of the natural variability of cob buildings hygric and thermal properties at material scale: Influence of plants add-ons.* Construction and Building Materials, 2022. **342**: p. 127922.